NASA/CR–2001–210852

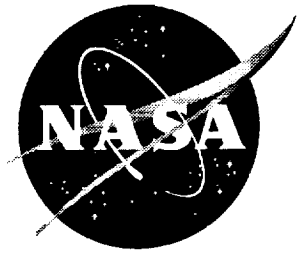

Inviscid Flow Computations of Two '07 Mars Lander Aeroshell Configurations Over a Mach Number Range of 2 to 24

Ramadas K. Prabhu
Lockheed Martin Engineering & Sciences Company, Hampton, Virginia

April 2001

The NASA STI Program Office ... in Profile

Since its founding, NASA has been dedicated to the advancement of aeronautics and space science. The NASA Scientific and Technical Information (STI) Program Office plays a key part in helping NASA maintain this important role.

The NASA STI Program Office is operated by Langley Research Center, the lead center for NASA's scientific and technical information. The NASA STI Program Office provides access to the NASA STI Database, the largest collection of aeronautical and space science STI in the world. The Program Office is also NASA's institutional mechanism for disseminating the results of its research and development activities. These results are published by NASA in the NASA STI Report Series, which includes the following report types:

- TECHNICAL PUBLICATION. Reports of completed research or a major significant phase of research that present the results of NASA programs and include extensive data or theoretical analysis. Includes compilations of significant scientific and technical data and information deemed to be of continuing reference value. NASA counterpart of peer-reviewed formal professional papers, but having less stringent limitations on manuscript length and extent of graphic presentations.

- TECHNICAL MEMORANDUM. Scientific and technical findings that are preliminary or of specialized interest, e.g., quick release reports, working papers, and bibliographies that contain minimal annotation. Does not contain extensive analysis.

- CONTRACTOR REPORT. Scientific and technical findings by NASA-sponsored contractors and grantees.

- CONFERENCE PUBLICATION. Collected papers from scientific and technical conferences, symposia, seminars, or other meetings sponsored or cosponsored by NASA.

- SPECIAL PUBLICATION. Scientific, technical, or historical information from NASA programs, projects, and missions, often concerned with subjects having substantial public interest.

- TECHNICAL TRANSLATION. English-language translations of foreign scientific and technical material pertinent to NASA's mission.

Specialized services that help round out the STI Program Office's diverse offerings include creating custom thesauri, building customized databases, organizing and publishing research results... even providing videos.

For more information about the NASA STI Program Office, see the following:

- Access the NASA STI Program Home Page at ***http://www.sti.nasa.gov***

- E-mail your question via the Internet to help@sti.nasa.gov

- Fax your question to the NASA STI Help Desk at (301) 621-0134

- Phone the NASA STI Help Desk at (301) 621-0390

- Write to:
  NASA STI Help Desk
  NASA Center for AeroSpace Information
  7121 Standard Drive
  Hanover, MD 21076-1320

NASA/CR–2001–210852

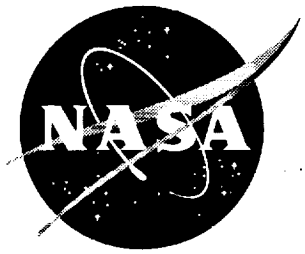

Inviscid Flow Computations of Two '07 Mars Lander Aeroshell Configurations Over a Mach Number Range of 2 to 24

Ramadas K. Prabhu
Lockheed Martin Engineering & Sciences Company, Hampton, Virginia

National Aeronautics and
Space Administration

Langley Research Center
Hampton, Virginia 23681–2199

Prepared for Langley Reseach Center
under contract NAS1-00135

April 2001

Available from the following:

NASA Center for AeroSpace Information (CASI)
7121 Standard Drive
Hanover, MD 21076–1320
(301) 621–0390

National Technical Information Service (NTIS)
5285 Port Royal Road
Springfield, VA 22161–2171
(703) 487–4650

Summary

This report documents the results of an inviscid computational study conducted on two aeroshell configurations for a proposed '07 Mars Lander. The aeroshell configurations are asymmetric due to the presence of tabs at the maximum diameter location. The purpose of these tabs was to change the pitching moment characteristics so that the aeroshell will trim at a non-zero angle-of-attack and produce a lift-to-drag ratio of approximately -0.25. This is required in the guidance of the vehicle on its trajectory. One of the two configurations is called the *shelf* and the other is called the *tab*. The unstructured grid software FELISA with the equilibrium Mars gas option was used for these computations. The computations were done for six points on a preliminary trajectory of the '07 Mars Lander at nominal Mach numbers of 2, 3, 5, 10, 15, and 24. Longitudinal aerodynamic characteristics namely lift, drag, and pitching moment were computed for 10, 15, and 20 degrees angle-of-attack. The results indicated that two configurations have very similar aerodynamic characteristics, and provide the desired trim L/D of approximately -0.25.

Nomenclature

C_A	Axial force coefficient
C_D	Drag coefficient
C_L	Lift coefficient
C_N	Normal force coefficient
C_m	Pitching moment coefficient about the point (0.0, 0.0, -0.8659)
C_p	$(p - p_\infty)/q_\infty$, Pressure coefficient
L/D	C_D/C_L, Lift-to-drag ratio
l_{ref}	Reference length for pitching moment (=4.05 m.)
M_∞	Freestream Mach number
p	Static pressure
p_∞	Freestream static pressure
q_∞	$\rho_\infty U_\infty^2/2$, Freestream dynamic pressure
S_{ref}	Reference area (=12.882 sq. m.)
T_∞	Freestream temperature (Kelvin)
U_∞	Freestream velocity (m/s)
x, y, z	Cartesian co-ordinates of a given point; (The origin is at the nose, with the x-axis in the vertical direction, the y-axis in the spanwise direction, and the z-axis in the axial direction pointing into the stream.)
ρ_∞	Freestream density (kg/m^3)
α	angle-of-attack (degrees)

Introduction

It has been proposed to use a passive device like a tab on the aeroshell for the '07 Mars lander to trim at a non-zero angle-of-attack, and use the non-zero lift-to-drag for guiding. In an effort aimed at arriving at a suitable aeroshell configuration for the '07 Mars lander, an extensive computational study was done (see

[1]), and the aerodynamic characteristics of several potential candidate configurations were computed. As a result of that study two configurations were selected for further study. These configurations are called the *shelf* and the *tab*. The maximum diameter of the aeroshell was increased form 3.75m (in the earlier study) to 4.05m. Since the present computations are inviscid, the size of the body does not affect the aerodynamic coefficients.

Unstructured grid technology is known to provide quick and reliable CFD solutions for complex configuration, particularly for hypersonic flows. Among the widely used unstructured grid software packages in use are the FELISA ([2] and [3]) and the TetrUSS ([4]) systems. In the Aerothermodynamics Branch (AB) at NASA Langley Research Center, FELISA grid generators and inviscid flow solvers have been used extensively for the computation of flow over complex vehicles, see for example [5] & [6]. FELISA flow solvers, being inviscid, have the obvious limitations; because of the absence of a boundary layer there is no skin friction and hence, there are no flow separation effects. For lifting bodies the inviscid flow solvers generally yield good results for normal force and pitching moment as long as there is no significant flow separation on the body. For a blunt body like the '07 Mars lander aeroshell, under hypersonic flow conditions the aerodynamic loads are primarily due to the pressures on the forebody, and the effects of skin friction are negligible. Although there is a fully separated flow over the aftbody, under hypersonic flow conditions the aftbody pressures are small, and contribute little to the aerodynamics loads. It is therefore expected that inviscid hypersonic flow computations would yield reliable results for the present case.

This paper presents the results of an inviscid computational study on the two aeroshell configurations of the '07 Mars lander using the unstructured grid software FELISA with the equilibrium Mars gas option. As noted earlier, these two configurations are the outcome of an extensive study [1] done to arrive at a suitable modification to the shape of the aeroshell. As in the earlier cases, only the forebodies of these configurations are simulated in the computations, and the aftbodies are ignored. Further, since the aeroshell has a plane of symmetry and only symmetric flow conditions are considered, only one half of the aeroshell is considered in the present study. The present study was done for nominal Mach numbers of 2, 3, 5, 10, 15, and 24 with freestream conditions on a preliminary trajectory of the '07 Mars lander. Computations were done for three angles-of-attack namely 10, 15, and 20 degrees. Computed pitching moment and drag coefficients and the lift-to-drag ratios are presented in this paper along with the C_D and L/D for trim conditions.

The FELISA Software

The grid generation and the flow computations of the present study were done using the unstructured grid software FELISA. This software package has been successfully used for extensive grid generation and hypersonic flow computations in Earth atmosphere (see [3], [5] & [6]). More recently, FELISA was used in the screening of several candidate aeroshell configurations for the '07 Mars lander [1].

The grid generation part of FELISA consists of a code for generating a surface triangulation, and a code for discretization of the computational domain using tetrahedral elements. The surface triangulation code employs the advancing front technique, and the volume discretization code employs the Delaunay approach. The FELISA software has two sets of flow solvers—one applicable for transonic flows and the other for hypersonic flows. Further, the hypersonic flow solver has options for perfect gas air, equilibrium air, equilibrium Mars gas (0.97 CO_2 and 0.03 N_2 by mass), CF_4 gas, CO_2 gas, and a finite rate Mars gas. The hypersonic flow solver with the equilibrium Mars gas option was used in the present study. Several post-processing codes, including the one to compute the aerodynamic coefficients by integrating the surface pressures, are parts of the FELISA software. More information on FELISA software may be found in references [2] and [3].

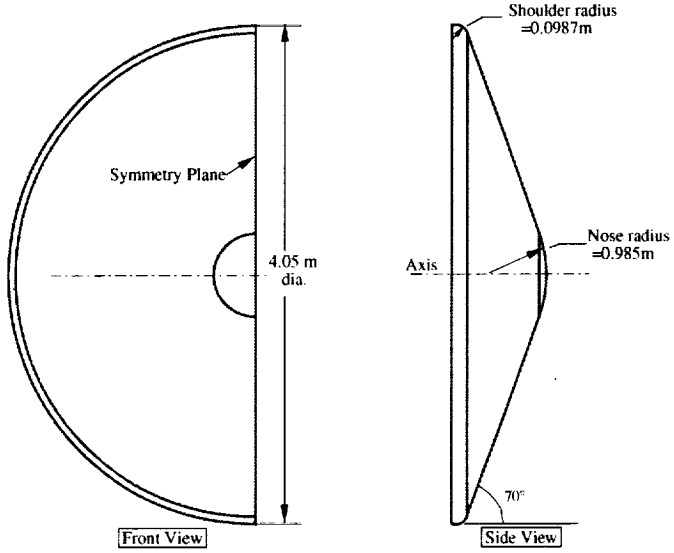

Figure 1: The geometry of the baseline '07 Mars lander aeroshell

Geometry

The baseline '07 Mars lander aeroshell is a 4.05m diameter blunt conical forebody with a 70-deg. half-cone angle. The nose radius of 0.985m and the shoulder radius is 0.0978m. Figure 1 shows the geometrical details of the baseline configuration. The reference quantities used to non-dimensionalize the aerodynamic loads are as follows:

Reference area, S_{ref}:	12.882 sq. m.
Reference length for pitching moment, l_{ref}:	4.05 m.
Pitching moment reference point:	on the axis, 0.8659 m. behind the nose.

This baseline shape being symmetric would trim at $\alpha = 0$ degrees with an L/D value of 0.0. In order to get the required L/D at the trim angle-of-attack, two modifications were made to the baseline shape of the vehicle. One of these configurations is designated WF-2.5-2.286-70 and the other is designated WF-1.9-2.286-80. In this paper, these are referred to as the *shelf* and the *tab* configurations, respectively. Figures 2 and 3 show the geometrical details of these two configurations. The modification to the baseline shape in the *shelf* configuration is an extension of the conical part of the aeroshell. The total width of the tab is 2.5m and its height is 0.261m. The *tab* configuration has the tab canted forward so that it makes an angle of 10 degrees with the conical part of the aeroshell. The total width of the tab in this case is 1.9m, and its projected height is 0.261m.

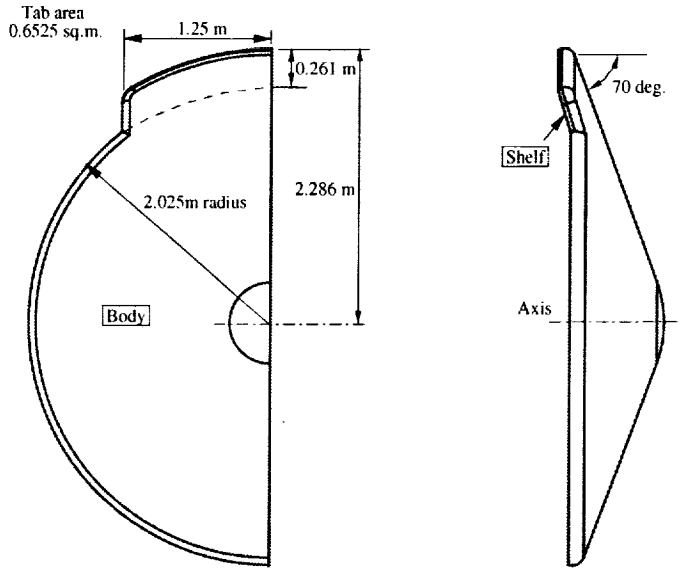

Figure 2: The WF-2.5-2.286-70 (*shelf*) configuration

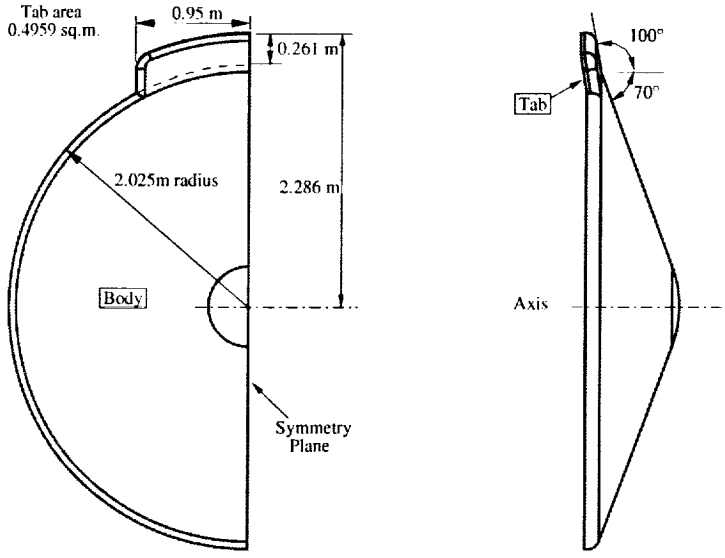

Figure 3: The WF-1.9-2.286-80 (*tab*) configuration

Grids

As noted before, only one half of the body is simulated in the present computations. The geometrical information of these configurations was available in the form of IGES files. These IGES files were processed using the GridTool [7] software. The computational domain was chosen to be sufficiently large with the surfaces of the bounding box sufficiently away from the body so that, except for the exit plane, all the boundary surfaces were in the freestream flow. The computational domain was made small enough so that the volume within this domain not influenced by the body was small. Figure 4 shows the computational domain used for the *tab* configuration for Mach 24 computations. This is typical of the computational domains used in the present study. The minimum grid spacing was 3.0 cm for the grid used for Mach 2 computations, whereas it was 1.0 cm for the grid used for Mach 24 computations. These spacings were chosen such that there were 8–12 points between the body and the bow shock in front of it. This provided sufficient resolution of flow features in that region. Choosing the appropriate computational domain and specifying the grid spacings was done using GridTool. Finally, a set of FELISA data files required by the grid generator were created.

Using the data files and the FELISA surface triangulator, the surface triangulation was generated. The surface triangulation near the tab and the triangulation of the symmetry plane for the grid used for the *tab* configuration for Mach 24 computations are shown in Fig. 5. This grid has 54,160 points and 105,930 triangles on the entire body surface, and 8,195 points and 15,868 triangles on the symmetry plane. After the surface triangulation was done, the volume grid of tetrahedral elements was generated. The tetrahedral (volume) grid for this case (not shown) has over 1.66M points. A different grid was built for each Mach number case. The processing of the IGES files and grid generation was done on an SGI Octane computer with 2GB memory. Generation of surface triangulation took about 20–30 minutes and the volume grid generation required 3–4 hours on the SGI machine.

Flow Solution

The unstructured volume grids of tetrahedral elements grids were partitioned so that the flow computations could be done on a parallel computer using (typically) 32 processors. The FELISA hypersonic flow solver with the Mars gas option was used for all the flow computations. Each flow solution was started with the low-order option, and after a few hundred iterations, the higher-order option was turned on, and the solution was run to convergence. After every 100 iteration, the surface pressures were integrated, and the aerodynamic loads, namely the normal and the axial forces, and the pitching moment acting on the body were computed. The flow solution was assumed to be converged when these integrated loads remained essentially constant. This required 6,000–8,000 iterations, and 150–180 hours of CPU time. Aerodynamic loads obtained by integrating the surface pressures were non-dimensionalized in the conventional manner, and the aerodynamic coefficients namely, C_N, C_A, C_L, C_D, C_m, and L/D were obtained.

All the computations reported here were done for nominal freestream Mach numbers of 2, 3, 5, 10, 15, and 24, at 10, 15, and 20 degrees angle-of-attack. As shown in Fig. 4, the *tab* or the *shelf* is located on the lee side flow when the aeroshell is at a positive angle-of-attack. The freestream gas was assumed to be Mars atmospheric gas in chemical equilibrium. The freestream velocity, density, temperature, and Mach numbers correspond to points on a preliminary '07 Mars lander trajectory, and are shown in Table 1.

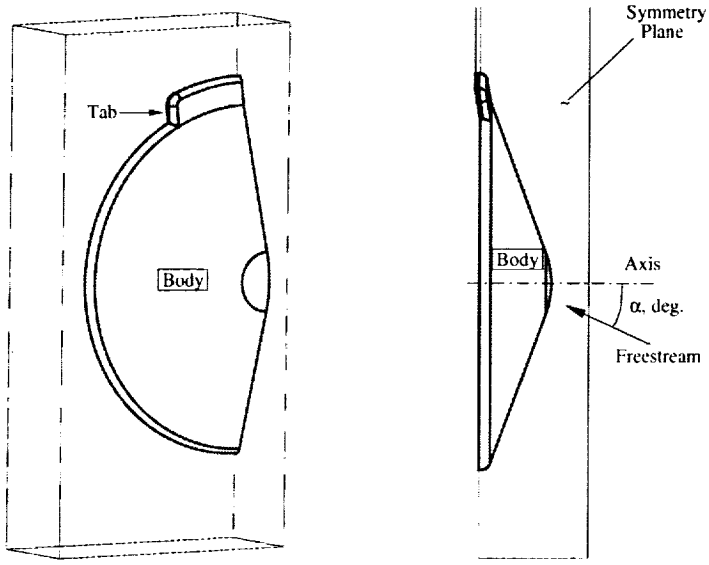

Figure 4: Computational domain for the *tab* configuration for Mach 24

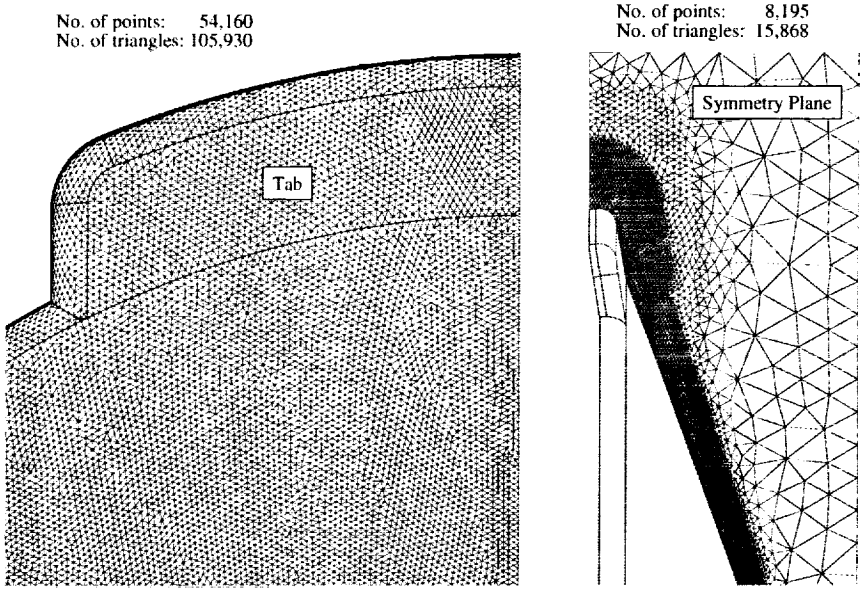

Figure 5: Surface and symmetry plane triangulation for the *tab* configuration

Velocity (*m/s*)	*Density* (kg/m^3)	*Temprature* (*Kelvin*)	*Mach Number*
494	5.756E-03	199.0	2.16
656	3.788E-03	195.5	3.00
1072	1.916E-03	183.0	4.86
2117	1.293E-03	177.0	9.74
3167	1.089E-03	175.0	14.6
4920	4.150E-04	159.0	23.7

Table 1: Freestream conditions used in the present computations

Results and Discussion

The aerodynamic data from the present computations are listed in Tables 2 and 3. It should be recalled at this point that the present computations are inviscid; hence the skin friction and flow separation effects are absent. In the present case, the axial force coefficients are large due to the very high pressures on the blunt forebody. Absence of the skin friction in inviscid computations leads to somewhat lower axial forces. But the contribution of the skin friction to axial force in the present case is expected to be a small fraction of the total axial force. Further, since the boundary layer is absent, the effects of boundary layer separation (over the forebody) on the aerodynamic loads are also absent. This could become a factor for the *tab* configuration, where the tab surface makes an angle of 10 degrees with the body surface and there is a possibility of flow separation on the forebody. In the present computations, only the forebody is simulated and the aftbody is ignored. Hence the contributions of the pressures on the aftbody to the aerodynamic loads are absent in the present results. Inviscid flow solver cannot simulate the highly viscous dominated separated flow over the aftbody. At low Mach number conditions (Mach 2, for example), the pressures in the separated flow regions over the aftbody would be large, and contribute significantly to the axial force (see, for example, Gnoffo, et al. [8]). A base pressue correction to the present results would thus be necessary at lower Mach numbers. With increase in the freestream Mach number, the aftbody pressures become small, and their contribution to the aerodynamic characteristics becomes less significant.

The *shelf* configuration

The piching moment coefficient C_m, the drag coefficients C_D, and the lift-to-drag ratio L/D for the *shelf* configuration are summarized in Table 2, and are shown plotted versus angle-of-attack in Figures 6–8. The sonic lines on the symmetry plane for Mach number from 2 to 24 are shown in Fig. 9. This figure indicates that the flow on the lee side of the body is subsonic for Mach numbers up to 5. For Mach 10 and 15, the sonic lines are grazing the leeside surface. For Mach 24 this flow is completely supersonic.

The pitching moment coefficients plotted versus angle-of-attack in Fig. 6 show that for Mach numbers 2, 3, and 5 the curves exhibit a certain slope. For higher Mach numbers the slope is distinctly higher. This trend is related to the flow over the lee side going from subsonic to supersonic as the Mach number is incresed beyond 5. The variation of C_m with Mach number for the three angles-of-attack is shown in Fig. 10

The drag coefficient shown in Fig. 7. It can be seen that C_D decreases with increase in α. This is primarily due to the fact that C_D is essentially a component of the axial force coefficient which is also seen

Mach No.	α (*deg.*)	C_N	C_A	C_m	C_L	C_D	L/D
2.16	10	1.1224E-03	1.4335	1.3638E-02	-2.4782E-01	1.4119	-1.7552E-01
2.16	15	1.5095E-02	1.3963	2.3807E-03	-3.4681E-01	1.3526	-2.5640E-01
2.16	20	2.9289E-02	1.3429	-8.9081E-03	-4.3178E-01	1.2719	-3.3947E-01
3.00	10	-3.7356E-04	1.5271	1.6215E-02	-2.6555E-01	1.5038	-1.7658E-01
3.00	15	1.3861E-02	1.4825	4.9183E-03	-3.7031E-01	1.4356	-2.5795E-01
3.00	20	2.9214E-02	1.4157	-7.1237E-03	-4.5675E-01	1.3403	-3.4077E-01
4.86	10	-3.3359E-03	1.6177	2.0821E-02	-2.8420E-01	1.5925	-1.7845E-01
4.86	15	1.2610E-02	1.5543	8.9572E-03	-3.9010E-01	1.5046	-2.5927E-01
4.86	20	3.4455E-02	1.4572	-8.5949E-03	-4.6601E-01	1.3811	-3.3742E-01
9.74	10	-5.1924E-03	1.6791	2.6070E-02	-2.9669E-01	1.6527	-1.7952E-01
9.74	15	1.8672E-02	1.5853	6.2411E-03	-3.9227E-01	1.5361	-2.5537E-01
9.74	20	4.3275E-02	1.4773	-1.4206E-02	-4.6460E-01	1.4030	-3.3115E-01
14.6	10	-6.2425E-04	1.7059	2.3045E-02	-2.9684E-01	1.6799	-1.7670E-01
14.6	15	2.3127E-02	1.6037	3.5360E-03	-3.9273E-01	1.5550	-2.5255E-01
14.6	20	4.8280E-02	1.4910	-1.7460E-02	-4.6458E-01	1.4176	-3.2773E-01
23.7	10	3.7460E-03	1.7090	1.9132E-02	-2.9308E-01	1.6837	-1.7407E-01
23.7	15	2.6850E-02	1.6072	3.7447E-04	-3.9004E-01	1.5594	-2.5012E-01
23.7	20	5.1316E-02	1.4907	-1.9577E-02	-4.6163E-01	1.4184	-3.2547E-01

Table 2: Aerodynamic coefficients for *shelf* configuration

to decrease with increase in α; The normal force coefficient being small, contributes little to the C_D. At a given angle-of-attack, C_D increase with Mach number. The variation of C_D with Mach number for the three angles-of-attack is shown in Fig. 11

The lift-to-drag ratio (Fig. 8) increases negatively with increase in angle-of-attack and changes very little with Mach number. This can also be seen in the plot of L/D with Mach number (see Fig. 12).

The *tab* configuration

The piching moment coefficient, the drag coefficient, and the lift-to-drag ratio for the *tab* configuration are summarized in Table 3 and are shown plotted versus angle-of-attack in Figures 13–15. The sonic lines on the symmetry plane for Mach number from 2 to 24 for the *tab* configuration is shown in Fig. 16. As in the case of the *shelf* configuration, the flow on the lee side is subsonic for Mach numbers up to 5. For Mach 10 and 15, the sonic lines are grazing the leeside surface. For Mach 24 the flow is completely supersonic.

The pitching moment coefficients plotted versus angle-of-attack in Fig. 13 show that for Mach numbers 2, 3, and 5 the curves exhibit a certain slope; for higher Mach numbers the slope is distinctly higher. This trend is closely related to the flow over the lee side going from subsonic to supersonic as the Mach number is incresesd beyond 5. The trends are similar to those of the *shelf* configuration. The variation of C_m with Mach number for the three angles-of-attack is shown in Fig. 17

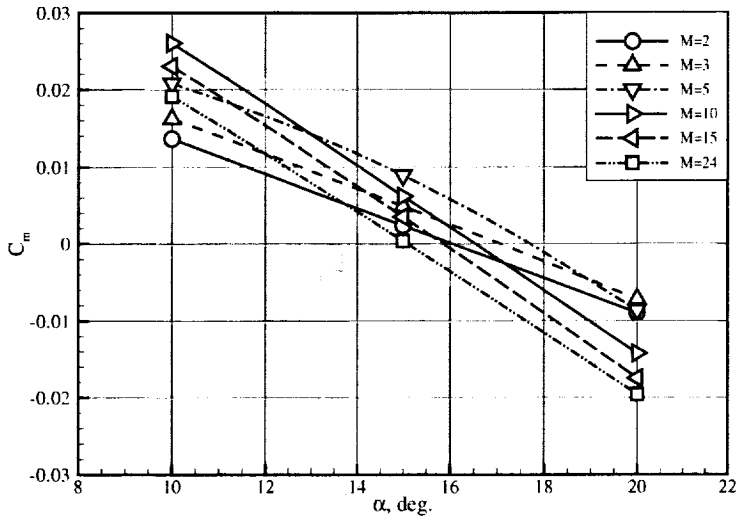

Figure 6: Pitching moment coefficient for the *shelf* configuration

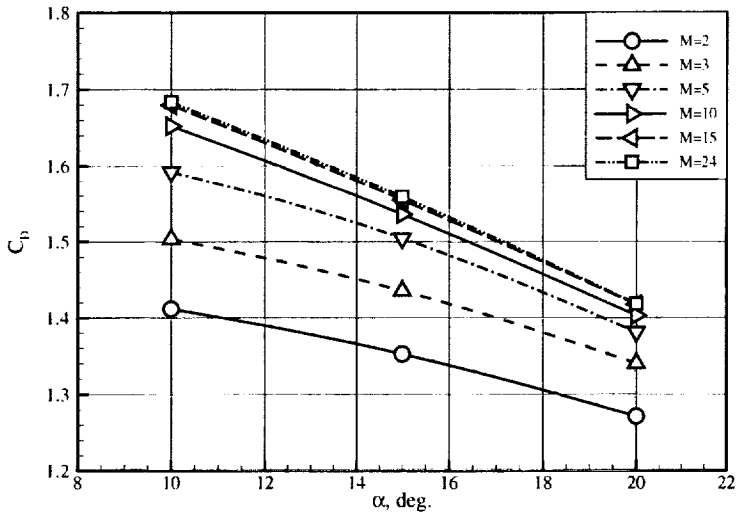

Figure 7: Drag coefficient for the *shelf* configuration

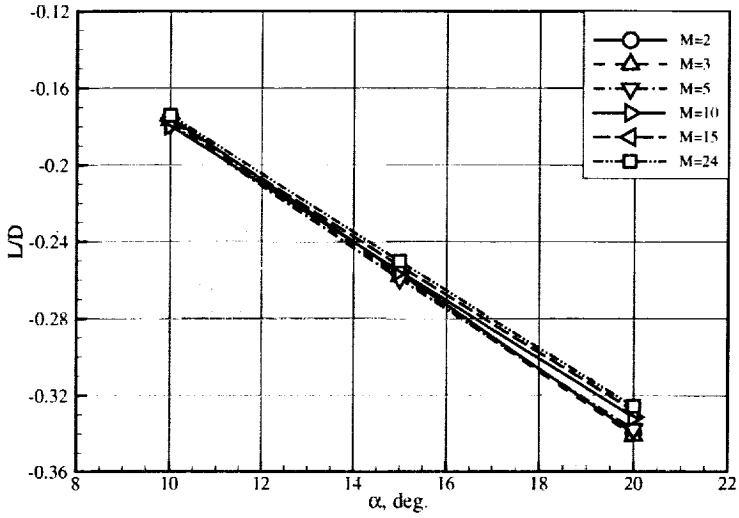

Figure 8: Lift-to-drag ration for the *shelf* configuration

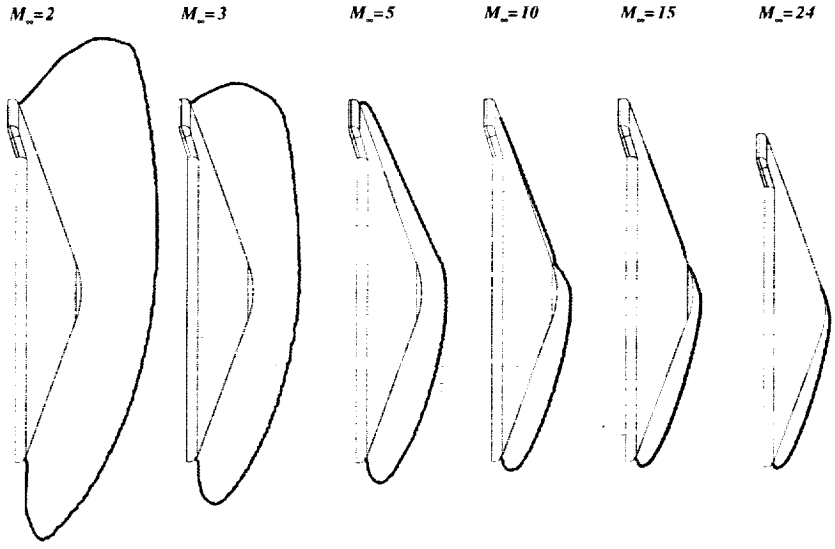

Figure 9: Symmetry plane sonic lines for the *shelf* configuration

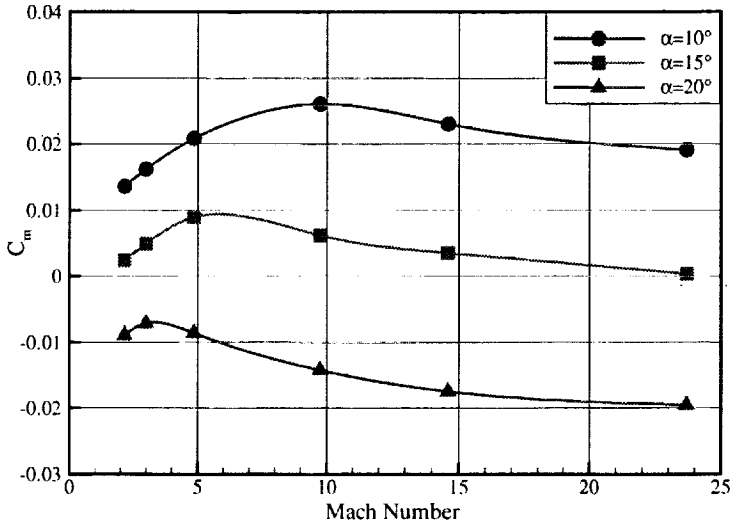

Figure 10: Pitching moment coefficient for the *shelf* configuration

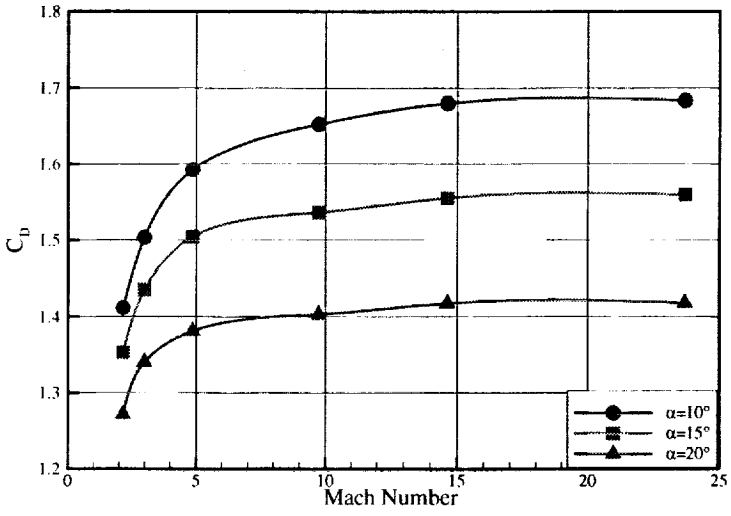

Figure 11: Drag coefficient for the *shelf* configuration

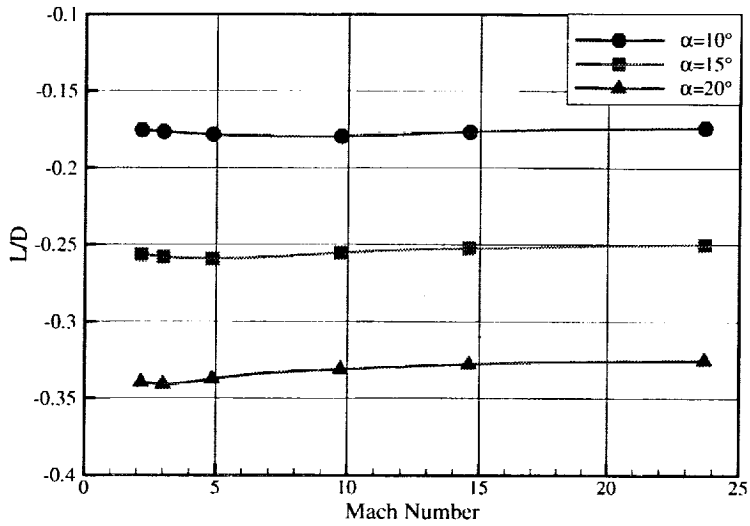

Figure 12: Lift-to-drag ratio for the *shelf* configuration

The drag coefficient is shown plotted in Fig. 14. Here again, with minor difference, the drag coefficient shows trends similar to those of the *shelf* configuration. At a given angle-of-attack, C_D increase with Mach number. The variation of C_D with Mach number for the three angles-of-attack is shown in Fig. 19

The lift-to-drag ratio (Fig. 15) increases negatively with increase in angle-of-attack and changes very little with Mach number. This can also be seen in the plot of L/D with Mach number (see Fig. 18).

The trim values

The values of angle-of-attack, L/D, and C_D at the trim condition (where C_m=0.0) for each Mach number were extracted for the two configuration, and are shown Figs. 20 to 22. It should be recalled here that the C_D values do not include the contribution due to the aftbody pressure. This contribution is significant at low Mach numbers. Gnoffo, et. al. [8] have shown that for Mars Pathfinder probe, at Mach 2 and α =2 degrees the contribution of the aftbdody pressures to the drag is of the order of 20%. This contribution decreases with increase in Mach number, and becomes negligible at Mach 24. The base pressure also affects the C_m, although to a lesser extent.

At low Mach numbers, the *shelf* and the *tab* have nearly the same trim angle, see Fig. 20. At Mach numbers higher than 5, the *shelf* configuration shows a reduction in the trim angle-of-attack. At Mach 24, the trim angle-of-attack for the *shelf* is 15.1 degrees whereas for the *tab* configuration, it is 17.9 degrees. The lift-to-drag values for the two configurations also show similar trend. At low Mach numbers the two configurations have the same L/D values. At Mach number higher than 5, the L/D of the *shelf* configuration becomes progressively less negative. At Mach 24, the *shelf* has an L/D of -0.252, whereas the *tab* has an L/D of -0.289. The trim C_D values are shown in Fig. 22.

The trim L/D values vary from -0.25 to -0.30 for both configurations over the Mach number range. Thus,

Mach No.	α *(deg.)*	C_N	C_A	C_m	C_L	C_D	L/D
2.16	10	1.1522E-02	1.4222	1.0371E-02	-2.3562E-01	1.4026	-1.6799E-01
2.16	15	2.3699E-02	1.3898	8.0339E-04	-3.3682E-01	1.3486	-2.4976E-01
2.16	20	3.6066E-02	1.3420	-8.6772E-03	-4.2510E-01	1.2734	-3.3383E-01
3.00	10	1.0829E-02	1.5145	1.3049E-02	-2.5233E-01	1.4934	-1.6896E-01
3.00	15	2.3149E-02	1.4758	3.7868E-03	-3.5960E-01	1.4315	-2.5121E-01
3.00	20	3.6644E-02	1.4143	-6.1467E-03	-4.4928E-01	1.3415	-3.3490E-01
4.86	10	7.9112E-03	1.6068	1.9206E-02	-2.7123E-01	1.5838	-1.7125E-01
4.86	15	2.2278E-02	1.5482	9.9382E-03	-3.7918E-01	1.5012	-2.5259E-01
4.86	20	4.2845E-02	1.4535	-6.1182E-03	-4.5687E-01	1.3805	-3.3094E-01
9.74	10	3.1026E-03	1.6835	3.3969E-02	-2.8928E-01	1.6585	-1.7443E-01
9.74	15	2.7832E-02	1.5833	1.2081E-02	-3.8290E-01	1.5366	-2.4920E-01
9.74	20	5.1379E-02	1.4721	-8.7823E-03	-4.5521E-01	1.4009	-3.2494E-01
14.6	10	1.0174E-02	1.7076	2.7858E-02	-2.8650E-01	1.6834	-1.7019E-01
14.6	15	3.1947E-02	1.6129	1.0036E-02	-3.8659E-01	1.5662	-2.4683E-01
14.6	20	5.5452E-02	1.5010	-1.0386E-02	-4.6126E-01	1.4294	-3.2269E-01
23.7	10	1.4970E-02	1.7220	2.6965E-02	-2.8438E-01	1.6990	-1.6738E-01
23.7	15	3.5312E-02	1.6260	1.0652E-02	-3.8686E-01	1.5800	-2.4481E-01
23.7	20	5.7637E-02	1.5120	-8.2727E-03	-4.6314E-01	1.4410	-3.2141E-01

Table 3: Aerodynamic coefficients for *tab* configuration

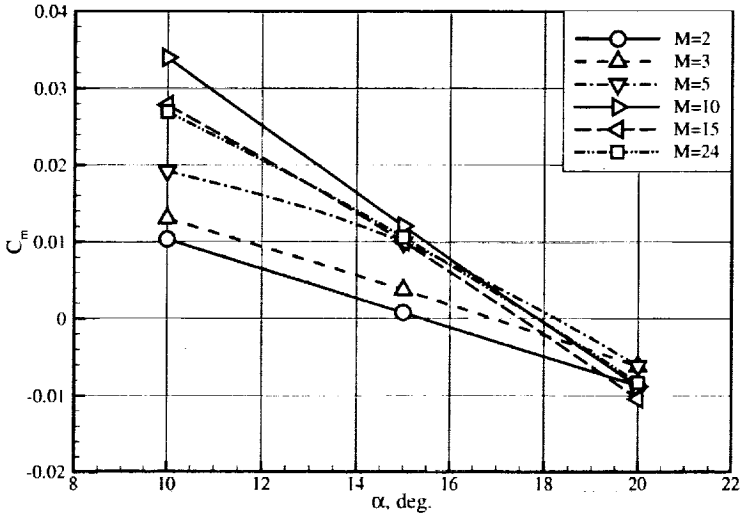

Figure 13: Pitching moment coefficient for the *tab* configuration

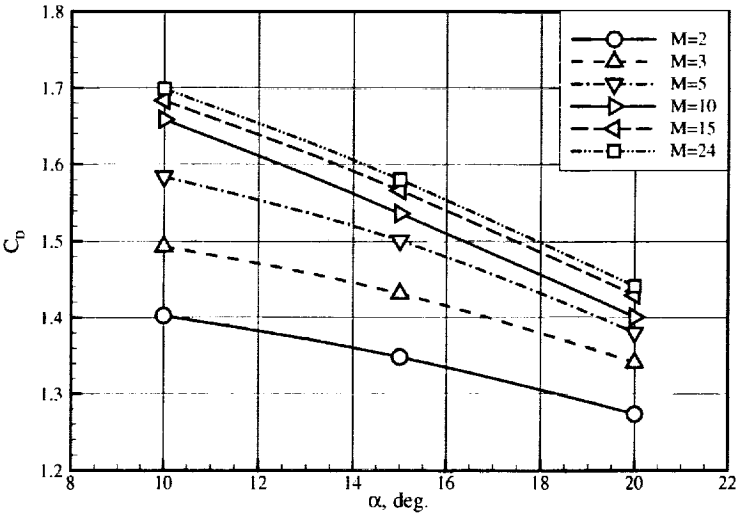

Figure 14: Drag coefficient for the *tab* configuration

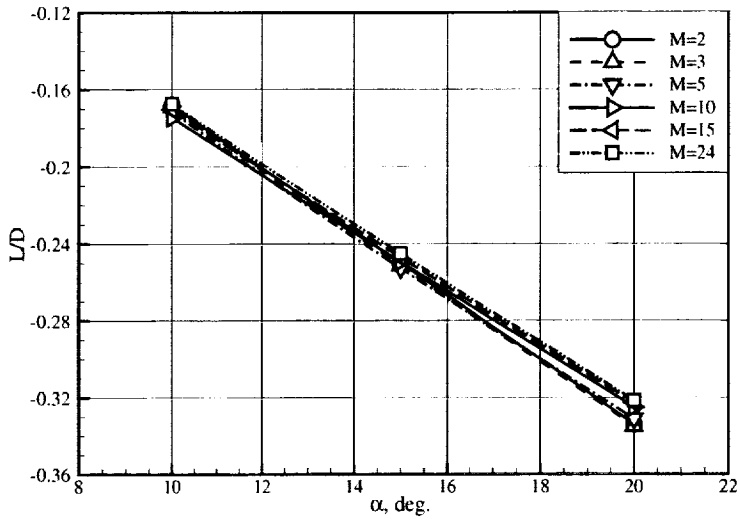

Figure 15: Lift-to-drag ration for the *tab* configuration

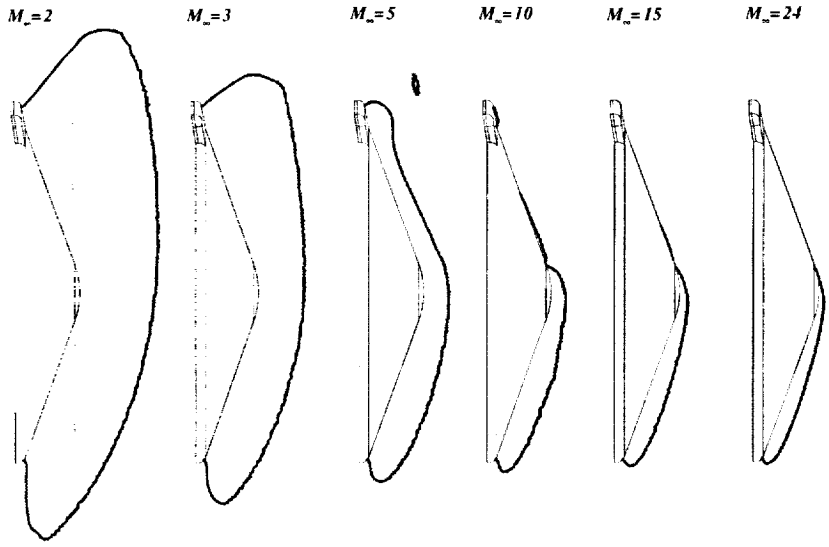

Figure 16: Symmetry plane sonic lines for the *tab* configuration

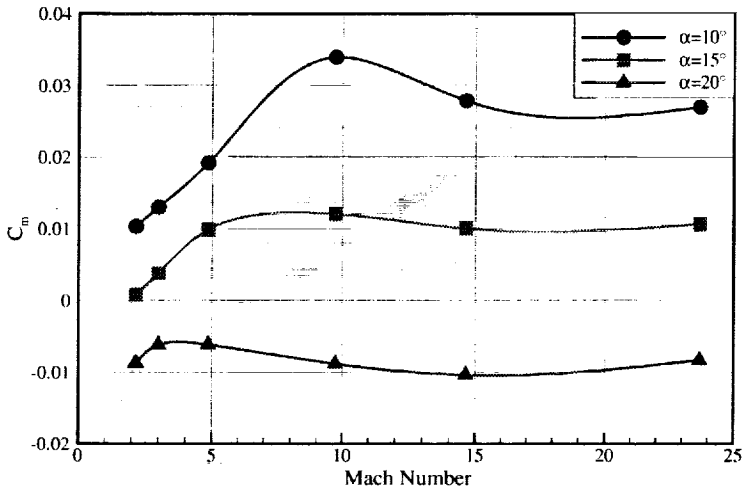

Figure 17: Pitching moment coefficient for the *tab* configuration

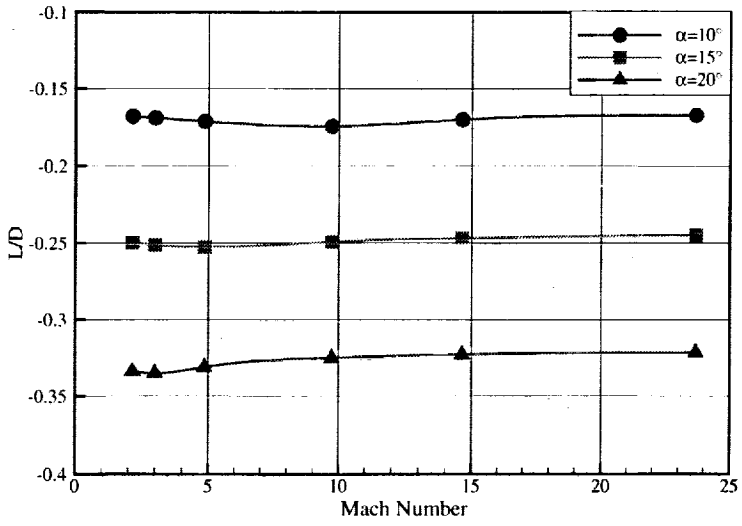

Figure 18: Lift-to-drag ratio for the *tab* configuration

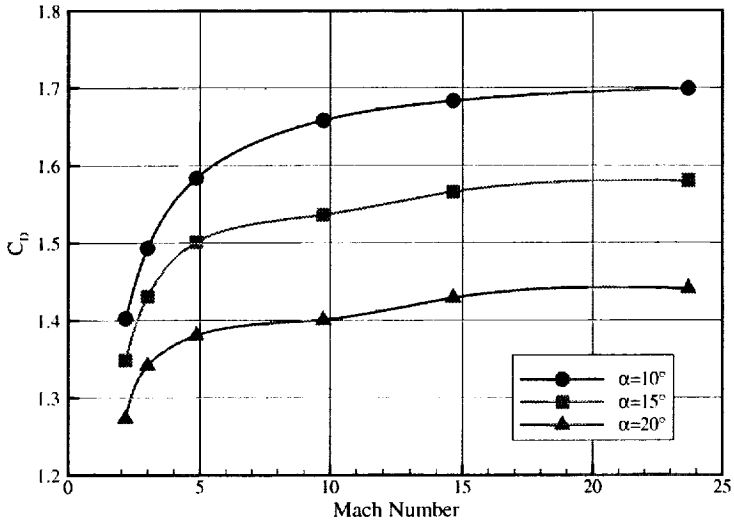

Figure 19: Drag coefficient for the *tab* configuration

the desired L/D of -0.25 is reasonably obtained. Some fine tuning of the tab widths is possible to adjust the trim angle-of-attack and trim L/D, if required. Note that the *tab* configuration has the larger trim angle-of-attack and a more negative trim L/D than the *shelf* configuration at the higher Mach numbers even though it has the smaller tab area. This result is due to the formation of a shock with greater tab surface pressure at Mach numbers of 10 and greater for the canted tab. Pressure contours along the leeward centerline at 15 degree angle-of-attack are shown in Figures 23 and 24 for the *shelf* configuration and Figures 25 and 26 for the *tab* configuration. The formation of a shock in front of the canted tab for the *tab* configuration is evident beginning at Mach 10. Note from Figures 9 and 16 that the flow over the leeward side is supersonic as the sonic line shifts to the forward hemispherical region at Mach 10, whereas the sonic line attaches at the aft corner with subsonic flow for the lower Mach numbers. Since the tab is not canted (in line with the conic section) for the *shelf* configuration, there are only expansion fans visble in the contour plots at the tab trailing edge for this configuration.

Conclusions

This paper documents the results of a computational study done on two aeroshell configurations of a proposed '07 Mars lander. These two configurations are designated the *shelf* and the *tab*, and are simple modifications to the baseline geometry. FELISA unstructured grid software was used for the grid generation and flow computations, and the inviscid longitudinal aerodynamic characteristics were computed for nominal Mach numbers of 2, 3, 5, 10, 15, and 24 at angles of attack of 10, 15, and 20 degrees. The freestream conditions corresponded to those on a preliminary trajectory of the '07 Mars lander. The freestream gas was assumed to be Mars atmospheric gas in equilibrium. Both configurations exhibited stable pitching moment characteristics, and yielded the desired lift-to-drag ratio of approximately -0.25 at the trim angle-of-attack.

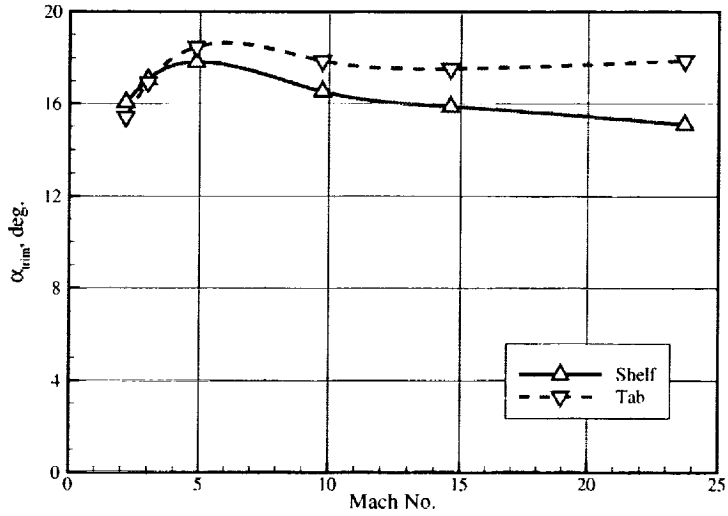

Figure 20: Trim angle-of-attack for the *shelf* and the *tab* configurations

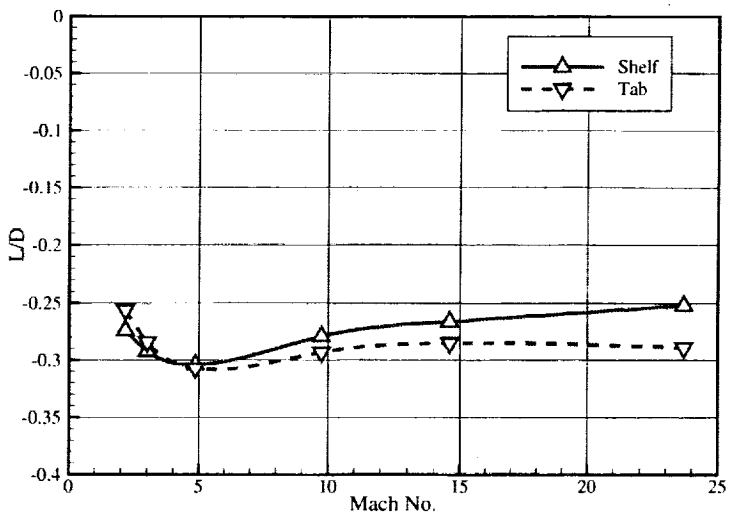

Figure 21: Trim lift-to-drag ratio for the *shelf* and the *tab* configurations

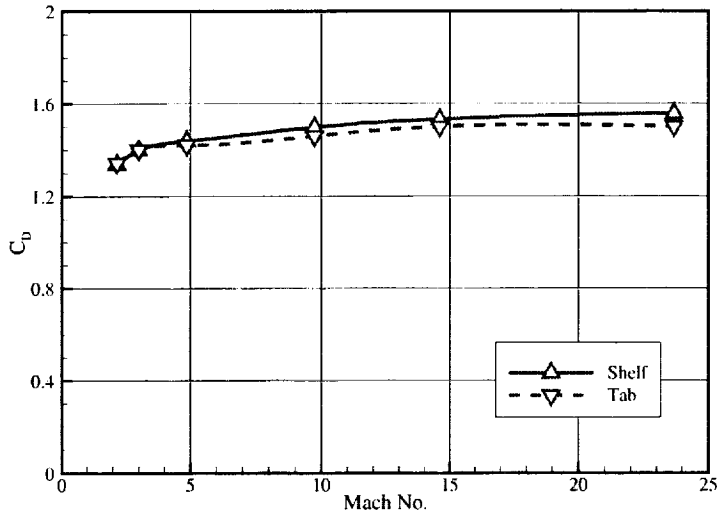

Figure 22: Trim drag coefficient for the *shelf* and the *tab* configurations

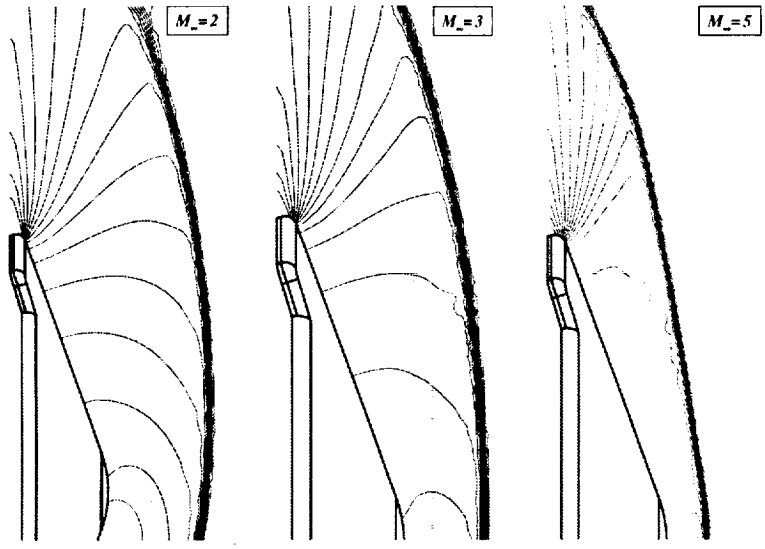

Figure 23: C_p contours for the *shelf* configuration for M=2, 3, & 5, α=15 deg.

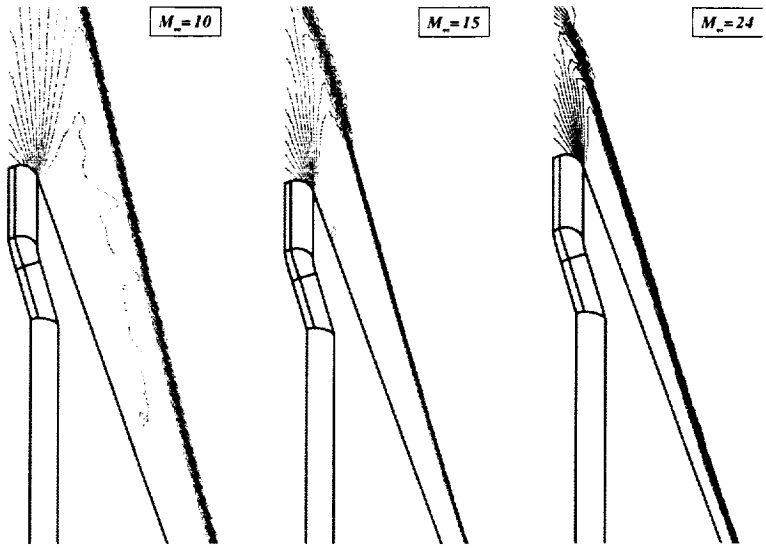

Figure 24: C_p contours for the *shelf* configuration for M=10, 15, & 24, α=15 deg.

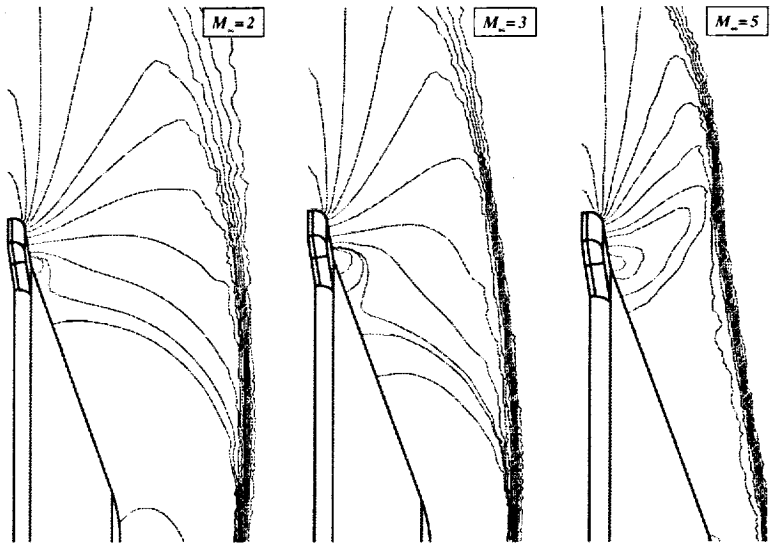

Figure 25: C_p contours for the *tab* configuration for M=2, 3, & 5, α=15 deg.

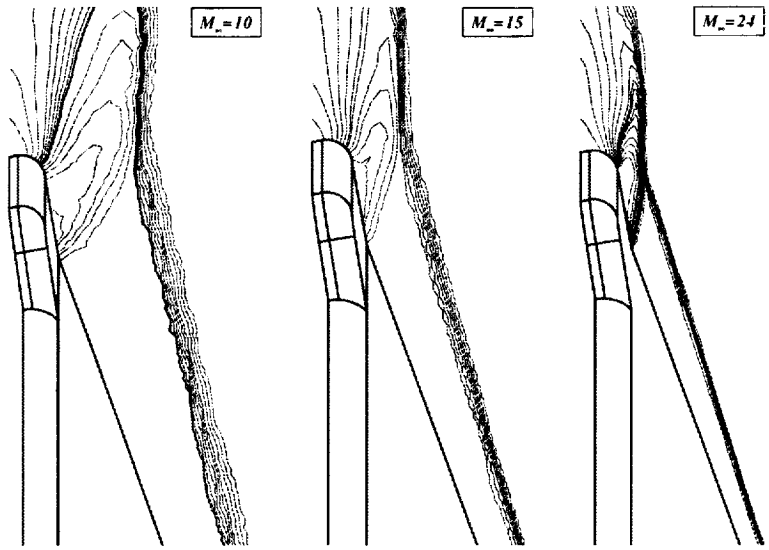

Figure 26: C_p contours for the *tab* configuration for M=10, 15, & 24, α=15 deg.

Acknowledgments

The author wishes to express his gratitude to Dr. K. Sutton of the Aerothermodynamics Branch (AB), NASA Langley Research Center for many helpful discussions during the course of this work. The work described herein was performed at Lockheed Martin Engineering & Sciences in Hampton, Virginia, and was supported by the AB, NASA Langley Research Center under the contract NAS1-00135. The technical monitor was Mr. K.J. Weilmuenster.

References

[1] Prabhu, R.K.: "Inviscid Flow Computations of Several Aeroshell Configurations for a '07 Mars Lander" NASA CR-2001-210851, April 2001.

[2] Peiro, J., Peraire, J., and Morgan, K.: "FELISA System Reference Manual and User's Guide," Tech. Report, University College of Swansea, Swansea, U.K., 1993.

[3] Bibb, K.L, Peraire, J., and Riley, C.J.: "Hypersonic Flow Computaions on Unstructure Meshes," AIAA 97-0625, Presented at the 35th Aerospace Sciences Meeting and Exhibit, Janaury 6-9, 1997, Reno. NV.

[4] Frink, N.T., Pirzadeh, S., and Parikh, P.: "An Unstructured-Grid Software System for Solving Complex Aerodynamic Problems," NASA CP-3291, pp. 289-308, May 9-11, 1995.

[5] Prabhu, R.K.: "An Inviscid Computational Study of an X-33 Configuration at Hypersonic Speeds" NASA CR-1999-209366, July 1999.

[6] Prabhu, R.K.: "Computational Study of a McDonnell Douglas Single-Stage-to-Orbit Vehicle Concept for Aerodynamic Analysis" NASA CR-20160, September 1996.

[7] Samereh, J.: "GridTool: A Surface Modeling and Grid Generation Tool," NASA CP 3291, May 1995.

[8] P.A. Gnoffo, K.J. Weilmuenster, R.D. Braun, and C.I. Cruz.: "Influence of Sonic-Line Location on Mars Pathfinder Probe Aerothermodynamic," *Journal of Spacecraft and Rockets*, Vol. 33, No. 2, March-April 1996.

REPORT DOCUMENTATION PAGE

Form Approved
OMB No. 0704–0188

1. AGENCY USE ONLY *(Leave blank)*	2. REPORT DATE	3. REPORT TYPE AND DATES COVERED
	April 2001	Contractor Report

4. TITLE AND SUBTITLE
Inviscid Flow Computations of Two '07 Mars Lander Aeroshell Configurations Over a Mach Number Range of 2 to 24

5. FUNDING NUMBERS
C NAS1-00135
WU 242-80-01-01

6. AUTHOR(S)
Ramadas K. Prabhu

7. PERFORMING ORGANIZATION NAME(S) AND ADDRESS(ES)
Lockheed Martin Engineering & Sciences Company
C/O NASA Langley Research Center
Hampton, VA 23681–2199

8. PERFORMING ORGANIZATION REPORT NUMBER

9. SPONSORING/MONITORING AGENCY NAME(S) AND ADDRESS(ES)
NASA Langley Research Center
Hampton, VA 23681–2199

10. SPONSORING/MONITORING AGENCY REPORT NUMBER
NASA/CR–2001–210852

11. SUPPLEMENTARY NOTES
Langley Technical Monitor: K. James Weilmuenster

12a. DISTRIBUTION/AVAILABILITY STATEMENT
Unclassified-Unlimited
Subject Category 02
Distribution: Nonstandard
Availability: NASA CASI (301) 621–0390

12b. DISTRIBUTION CODE

13. ABSTRACT ***(Maximum 200 words)***

This report documents the results of an inviscid computational study conducted on two aeroshell configurations for a proposed '07 Mars Lander. The aeroshell configurations are asymmetric due to the presence of the tabs at the maximum diameter location. The purpose of these tabs was to change the pitching moment characteristics so that the aeroshell will trim at a non-zero angle of attack and produce a lift-to-drag ratio of approximately -0.25. This is required in the guidance of the vehicle on its trajectory. One of the two configurations is called the *shelf* and the other is called the *tab*. The unstructured grid software FELISA with the equilibrium Mars gas option was used for these computations. The computations were done for six points on a preliminary trajectory of the '07 Mars Lander at nominal Mach numbers of 2, 3, 5, 10, 15, and 24. Longitudinal aerodynamic characteristics namely lift, drag, and pitching moment were computed for 10, 15, and 20 degrees angles of attack. The results indicated that the two configurations have aerodynamic characteristics that have very similar aerodynamic characteristics, and provide the desired trim L/D of approximately -0.25.

14. SUBJECT TERMS
Unstructured Grid CFD, Hypersonic Speeds, Mars Gas, Aerodynamic Loads

15. NUMBER OF PAGES
27

16. PRICE CODE
A03

17. SECURITY CLASSIFICATION OF REPORT	18. SECURITY CLASSIFICATION OF THIS PAGE	19. SECURITY CLASSIFICATION OF ABSTRACT	20. LIMITATION OF ABSTRACT
Unclassified	Unclassified	Unclassified	UL